# Accepted Manuscript

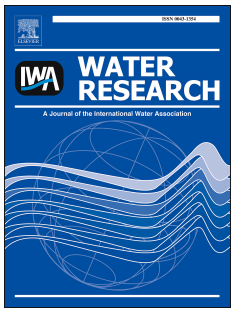


In-situ chemical oxidation of chlorendic acid by persulfate: Elucidation of the roles of adsorption and oxidation on chlorendic acid removal

Alannah Taylor, Nick Zrinyi, Stephen P. Mezyk, Jamie M. Gleason, Leah MacKinnon, Andrzej Przepiora, Anh Le-Tuan Pham

PII: S0043-1354(19)30574-3

DOI: https://doi.org/10.1016/j.watres.2019.06.061

Reference: WR 14817

To appear in: *Water Research*

Received Date: 23 March 2019

Revised Date: 11 June 2019

Accepted Date: 22 June 2019

Please cite this article as: Taylor, A., Zrinyi, N., Mezyk, S.P., Gleason, J.M., MacKinnon, L., Przepiora, A., Pham, A.L.-T., In-situ chemical oxidation of chlorendic acid by persulfate: Elucidation of the roles of adsorption and oxidation on chlorendic acid removal, *Water Research* (2019), doi: https://doi.org/10.1016/j.watres.2019.06.061.

This is a PDF file of an unedited manuscript that has been accepted for publication. As a service to our customers we are providing this early version of the manuscript. The manuscript will undergo copyediting, typesetting, and review of the resulting proof before it is published in its final form. Please note that during the production process errors may be discovered which could affect the content, and all legal disclaimers that apply to the journal pertain.

The final publication is available at Elsevier via https://doi.org/10.1016/j.watres.2019.06.061. © 2019. This manuscript version is made available under the CC-BY-NC-ND 4.0 license http://creativecommons.org/licenses/by-nc-nd/4.0/

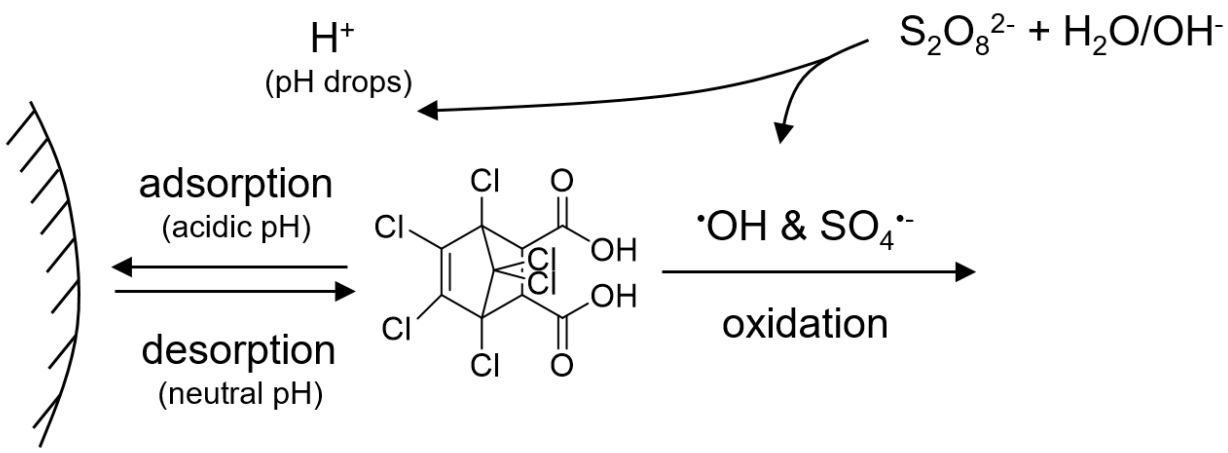


ACCEPTED MANUSCRIPT

ACCEPTED MANUSCRIPT

# In-Situ Chemical Oxidation of Chlorendic Acid by Persulfate: Elucidation of the Roles of Adsorption and Oxidation on Chlorendic Acid Removal

*Alannah Taylor[1], Nick Zrinyi[1], Stephen P. Mezyk[2], Jamie M. Gleason[2], Leah MacKinnon[3], Andrzej Przepiora[3] and Anh Le-Tuan Pham [4]**

[1]Department of Civil and Environmental Engineering, Carleton University
Ottawa, Ontario, Canada

[2]Department of Chemistry and Biochemistry, California State University at Long Beach
Long Beach, California, USA

[3]Geosyntec Consultants Inc.,
Guelph and Waterloo Offices, Ontario, Canada

[4]Department of Civil and Environmental Engineering, University of Waterloo
Waterloo, Ontario, Canada

*(Manuscript prepared for submission to Water Research)*

*Corresponding authors: Anh Le-Tuan Pham (email: anh.pham@uwaterloo.ca; phone: +1-519-888-4567 ext. 30337)

**Abstract**

The oxidation of chlorendic acid (CA), a polychlorinated recalcitrant contaminant, by heat-, mineral-, and base-activated persulfate was investigated. In pH 3 – 12 homogeneous (i.e., solid-free) solutions, CA was oxidized by $^{\bullet}OH$ and $SO_4^{\bullet-}$ radicals, resulting in a nearly stoichiometric production of $Cl^-$. The rate constants for the reaction between these radicals and CA were measured at different temperatures by electron pulse radiolysis, and were found to be $k_{OH}$ = (8.71 ± 1.67)×$10^7$ $M^{-1}s^{-1}$ and $k_{SO4}$ = (6.57 ± 0.83)×$10^7$ $M^{-1}s^{-1}$ at 24.5 ºC for $^{\bullet}OH$ and $SO_4^{\bullet-}$, respectively. CA was oxidized at much slower rates in solutions containing iron oxyhydroxide or aquifer soils, partially due to the adsorption of CA on these solids. To gain further insight into the effect of solids during *in-situ* remediation of CA, the adsorption of CA onto iron oxide, manganese dioxide, silica, alumina, and aquifer soils was investigated. The fraction of CA that was adsorbed on these materials increased as the solution pH decreased. Given that the solution pH can decrease dramatically in persulfate-based remedial systems, adsorption may reduce the ability of persulfate to oxidize CA. Overall, the results of this study provide important information about how persulfate can be used to remediate CA-contaminated sites. The results also indicate that the groundwater pH and geology of the subsurface could have a significant influence on the mobility of CA.

ACCEPTED MANUSCRIPT

40 **Graphical Abstract**

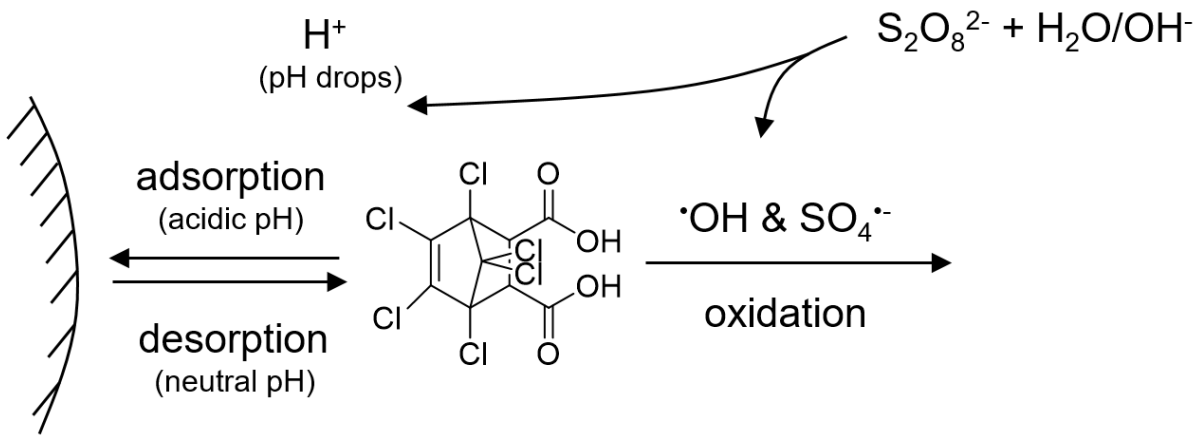


41

ACCEPTED MANUSCRIPT

## 1. Introduction

Chlorendic acid (1,4,5,6,7,7-hexachlorobicyclo[2.2.1]-hept-5-ene-2,3-dicarboxylic acid) is a polychlorinated organic compound used in multiple applications, including as a flame retardant, an intermediate in the synthesis of polymeric resins and corrosion-resistant materials, and an additive in extreme-pressure lubricants (NTP, 1987; IPCS, 1996). Commercially known as HET acid, chlorendic acid (CA) is synthesized via a Diels-Alder reaction between hexachloropentadiene and maleic anhydride. With a bridged ring and six Cl atoms (Figure S1 in the Supporting Information - SI), CA is structurally similar to the norbornene pesticides and flame retardants such as dieldrin, heptachlor, endosulfan and dechlorane plus. Some of these compounds, particularly dechlorane plus, have recently gained great attention based on their widespread presence in the environment (Sverko *et al*. 2011).

CA can enter the environment either via disposal of CA-containing wastes or as a transformation byproduct of chlorinated norbornenes (Cochrane and Forbes, 1974; Ying *et al.* 1986; Ying *et al*. 1988; Oman and Hynning, 1993). While the fate of CA in the environment is not well understood, the compound is potentially more mobile than its norbornene counterparts owing to its higher aqueous solubility ($C_w^s$ = 3.5 g/L (IPCS, 1998)), relatively hydrophilic nature (log $K_{ow}$ = 2.3 (IPCS, 1998)), and negative molecular charge at environmentally relevant pH values (the $pK_{a1}$ and $pK_{a2}$ of CA are 3.1 and 4.6, respectively (Hendrix *et al*., 1983)). The mobility of CA, however, can be influenced by its adsorption onto surfaces, a process that appears to be strongly controlled by the solution pH and surface properties. It has been observed that iron (hydr)oxide can adsorb CA, that more CA was adsorbed at pH 3.3 than at pH 7, and that the freshly-formed iron (hydr)oxide precipitates were better at adsorbing CA than the aged precipitates (Ying *et al.*, 1988). Bench-scale tests have shown that CA is very resistant to

biodegradation, suggesting that the natural attenuation of this compound in the environment would not occur to any appreciable extent (Hendrix *et al.*, 1983; Ying *et al.*, 1986). Considering CA's mobility and persistence, together with its potential toxicity (IPCS, 1998), remedial actions may be required for sites contaminated with CA.

This study investigates the degradation of CA by persulfate ($S_2O_8^{2-}$), an oxidant that is being increasingly used in advanced oxidation processes for water and wastewater treatment, and *in-situ* chemical oxidation (ISCO) for groundwater remediation (Huling and Pivetz, 2006; Tsitonaki et al., 2010; Siegrist et al., 2011; Drzewicz *et al.*, 2012; Lutze *et al.*, 2015; Bockzaj and Fernandes, 2017). Currently, there is very little information about the ability of $S_2O_8^{2-}$ to destroy CA. A few studies suggested that CA can be destroyed by ozone ($O_3$) (Stowell and Jensen, 1991), peroxymonosulfate ($HSO_5^-$) and $S_2O_8^{2-}$ (Shah *et al.*, 2016), $TiO_2$/UV (Boisa, 2013), and electrochemical-based advanced oxidation (Hermes and Knupp, 2015). The transformation of CA in those studies were attributed to reactions with hydroxyl ($^{\bullet}OH$) and sulfate ($SO_4^{\bullet-}$) radicals, suggesting that an activated persulfate-based process could be employed to treat CA-contaminated sites. We note that except for the $TiO_2$/UV system, the CA transformation in those studies took place in homogeneous (i.e., solid-free) solutions. It is thus unclear how this transformation would have been affected by the presence of surfaces, particularly iron-containing surfaces (e.g., Fe-containing suspended solids, soils, sediments). Because CA has a higher affinity toward iron surfaces at acidic pH (Ying *et al.*, 1988), *adsorptive* removal (rather than *oxidative* transformation) could be especially significant in persulfate-based treatment systems in which the solution pH decreases dramatically due to the decomposition of $S_2O_8^{2-}$. As such, after persulfate treatment the concentration of CA might rebound once the solution pH increases to the pre-treatment condition and CA desorbs from the minerals.

The overall objective of this study was to evaluate whether $S_2O_8^{2-}$-based ISCO could be effectively employed to remediate CA-contaminated sites. First, we assessed the reactivity of chlorendic acid with $^{\bullet}OH$ and $SO_4^{\bullet-}$ radicals by measuring their absolute reaction rate constants, $k_{OH}$ and $k_{SO4}$, using electron pulse radiolysis. We then studied the degradation of CA by $S_2O_8^{2-}$ in solid-free and solid-containing solutions, employing either synthetic materials or authentic groundwater and aquifer soils. To differentiate between the CA loss by adsorption and by transformation, the concentration of CA remained in the solution, the amount of CA adsorbed on the solid, and the production of chloride ($Cl^-$) were carefully monitored. The adsorption of CA on model minerals and an authentic aquifer soil was also investigated to gain insights into how adsorption can influence the fate of CA oxidation.

ACCEPTED MANUSCRIPT

## 2. Materials and methods

**2.1 Chemicals.** Silica ($SiO_2$, 35-60 mesh), aluminum oxide ($Al_2O_3$, ca. 150 mesh), iron(III)-oxyhydroxide ($Fe^{III}$-ox, 30-50 mesh), and manganese oxide ($MnO_2$) were obtained from Sigma Aldrich. Potassium persulfate ($K_2S_2O_8$) was purchased from VWR. All other chemicals, purchased from either Fisher Scientific or Sigma Aldrich, were of reagent grade and were used without further purification. All solutions were prepared using 18.2 MΩ·cm water from a Millipore System.

**2.2 Determination of reaction rate constants $k_{OH}$ and $k_{SO4}$.** The absolute rate constants for the reactions between CA and $^{\bullet}OH$ and $SO_4^{\bullet-}$ radicals at different temperatures were obtained using the linear accelerator (LINAC) electron pulse radiolysis system at the Radiation Laboratory, University of Notre Dame. This approach has the advantage of generating specific, isolated radicals through deposition energy into the solvent under well-established chemical conditions. The irradiation and transient absorption detection system has been described previously (Whitman *et al.*, 1996, Hug *et al*. 1999). Absolute radical yields (dosimetry) were determined using nitrogen oxide ($N_2O$)-saturated solutions of $1.00 \times 10^{-2}$ M potassium thiocyanate (KSCN) at $\lambda = 475$ nm, ($G\varepsilon = 5.2 \times 10^{-4}$ m$^2$ J$^{-1}$) with average doses of 3−8 Gy per 2−10 ns pulse (Buxton and Stuart, 1995), giving initial radical concentrations in the 2 – 6 μM range. For the room-temperature and 40$^{o}$C measurements, irradiations were performed on continuously flowed solutions that were first passed through a temperature-controlled condenser. By placing a thermocouple in the direct flow after irradiation the solution temperature was continuously measured and found to be stable to ± 0.3 $^{o}$C (Gleason *et al*., 2017). For the 70$^{o}$C measurements, static solutions in a temperature-controlled, sealed, cuvette were irradiated by the electron beam.

120 The temperature was stable to ± 0.2 $^{o}$C, but only a few kinetic traces could be obtained before
121 interference from irradiation products became significant.

122 For all $^{\bullet}$OH radical irradiation experiments, solutions were pre-saturated with $N_2O$ gas to
123 prevent air ingress, and to quantitatively convert the hydrogen atom and hydrated electrons
124 initially formed to the desired $^{\bullet}$OH radicals. (Buxton *et al*., 1988; Spinks and Woods, 1990).

125 Since the direct reaction of the $^{\bullet}$OH radical with CA did not give any suitable absorbance
126 change across the UV-visible spectrum, competition kinetics method based on $SCN^-$ was
127 utilized. The reaction of $^{\bullet}$OH with $SCN^-$ proceeds according to:

128 $^{\bullet}OH + SCN^- (+ SCN^-) \rightarrow OH^- + (SCN)_2^{-\bullet}$ $k_1 = 1.05 \times 10^{10}\ M^{-1}\ s^{-1}$ (Buxton *et al*., 1988) (1)

129 which will occur in competition with this radical's reaction with chlorendic acid (CA):

130 $^{\bullet}OH + CA \rightarrow$ products $k_2$ (2)

131 This competition can be directly solved to give the following analytical expression:

132 $$\frac{Abs^{o}(SCN)_2^{-\blacksquare}}{Abs(SCN)_2^{-\blacksquare}} = 1 + \frac{k_2[CA]}{k_1[SCN^-]} \quad (3)$$

133 where $Abs^{o}(SCN)_2^{-\bullet}$ is the $(SCN)_2^{-\bullet}$ yield (transient absorbance peak at 475 nm) in the absence of
134 any chlorendic acid, and $Abs(SCN)_2^{-\bullet}$ is the reduced yield when chlorendic acid is present. By
135 creating a transformed plot of the ratio of these absorbance intensities against the ratio of
136 concentrations for the competitors [CA]/[$SCN^-$] the second order rate constant ratio ($k_2/k_1$) can
137 be readily determined.

138 For $SO_4^{\bullet-}$ radical generation, aerated solutions containing 0.10 M $K_2S_2O_8$ were used at the
139 desired pH. The fast reduction of $S_2O_8^{2-}$ by the hydrated electron under these conditions ensures
140 quantitative production of $SO_4^{\bullet-}$ even in the presence of ambient dissolved oxygen (~250 μM)
141 (Buxton et al., 1988). By directly observing the change in the rate of decay of $SO_4^{\bullet-}$ radical's
142 absorbance at 450 nm, the kinetics of reaction (4) can be directly measured:

143 $SO_4^{\bullet-}$ + CA → products $k_4$ (4)

144 These kinetics were found to be pseudo-first-order, and therefore fitted with a single exponential
145 decay function:

146 $$Abs = Abs^o * e^{-k't} + B \quad (5)$$

147 where k' = $k_4$[CA] is the pseudo-first-order rate constant fitted, and B is a baseline adjustable
148 parameter. The fitted k' values were plotted against the CA concentration, with the fitted line
149 corresponding to the second-order rate constant of $k_4$.

150 **2.3 Treatment of chlorendic acid by heat-activated persulfate.** The experiments investigating
151 the degradation of CA by heat-activated $S_2O_8^{2-}$ were carried out in the dark, employing 16-mL
152 test tubes that contained 10-mL of reaction solution. Each solution initially contained 1 mM
153 $S_2O_8^{2-}$, 50 mM $Na_2SO_4$ (background electrolyte), and 0.1 mM CA. The concentration of CA in
154 this study was similar to those employed by others (Stowell and Jensen, 1991; Boisa, 2013;
155 Hermes and Knupp, 2015), and was representative of the CA concentrations that could be found
156 at CA-impacted sites (Ying *et al.*, 1986; Ying *et al.*, 1988). Some test tubes also contained 50
157 g/L $Fe^{III}$-ox. Solutions with initial pH values of 8.3 – 8.4 were buffered by 20 mM borate,
158 whereas solutions with initial pH values of 3.8 or 12.2 were unbuffered.

159 The thermal activation of $S_2O_8^{2-}$ was initiated by placing the test tubes in a water bath at T =
160 70 ºC. At pre-determined time intervals, 3 test tubes were sacrificed, and reactions were
161 immediately quenched in an ice bath. Subsequently, the samples were filtered through a 0.2-µm
162 filter membrane and analyzed for pH, $S_2O_8^{-}$, CA, and chloride ($Cl^-$) concentrations. To account
163 for the fraction of CA that was lost due to adsorption in the experiments involving $Fe^{III}$-ox, the
164 filtered $Fe^{III}$-ox particles were collected and added to a separate test tube containing 10 mL of pH
165 12 aqueous solution. This tube then was mixed end-over-end for 45 min. Subsequently, an

aliquot was subsampled from the tube, filtered, and analyzed for CA. Control experiments indicated that this extraction procedure usually recovered more than 90% of the CA that was pre-adsorbed onto $Fe^{III}$-ox surface.

**2.4 Adsorption of chlorendic acid onto minerals.** To gain insight into how aquifer minerals may affect the ability of $S_2O_8^{2-}$ to destroy CA during ISCO, the interaction between CA and $Fe^{III}$-ox, $MnO_2$, $SiO_2$, and $Al_2O_3$ was investigated. These solids were chosen to represent the Fe-, Mn-, Si-, and Al-containing minerals in the subsurface (e.g., aluminosilicates, ferrihydrite, Fe- and Mn-containing sands and clays). In the adsorption experiments, reaction solutions contained 50 g/L of a single type of solid, 0.1 mM CA, and 10 mM $Na_2SO_4$ (background electrolyte). The adsorption of CA in solution containing a lower concentration of $Fe^{III}$-ox (5 g/L) was also investigated. Aliquots of 1M NaOH or 1M $H_2SO_4$ were added to each test tube to obtain different initial pHs (these solutions did not contain any pH buffer), and the test tubes were mixed end-over-end at room temperature (22 ± 1 ºC). After 30 min, the pH of the suspension was measured, and an aliquot was taken out and filtered through a 0.2-μm syringe filter. Subsequently, the amount of CA in the filtrate was quantified. Although adsorption equilibrium may not have been attained within 30 min, the objective of this experiment was simply to examine how the solution pH influences adsorption affinity. Investigating adsorption kinetics, developing adsorption isotherm, or comparing the adsorption capacity among the solids were not the focus of this study.

**2.5 Experiments with groundwater and aquifer soil.** Experiments employing authentic samples of groundwater and aquifer soil were also conducted to further investigate the utility of $S_2O_8^{2-}$ for *in-situ* treatment of CA. The aquifer soils used in this study consisted mainly of sandy soils with the concentration of total iron (Fe) and organic carbon (OC) of approximately 10 g/kg

and 4g/kg, respectively. The groundwater contained approximately 55 mg/L of $Cl^-$, 30 mg/L of sulfate ($SO_4^{2-}$), 20 mg/L of calcium ($Ca^{2+}$), 3 mg/L of magnesium ($Mg^{2+}$), 10 mg/L of total dissolved iron, and 5 mg/L Total Organic Carbon (TOC). The pH of the groundwater was 5.8. The groundwater was amended with CA to obtain an initial concentration of 50 μM. To evaluate the affinity of CA towards the surface of the aquifer soils, an adsorption experiment similar to that described in section 2.4 was conducted.

Batch reactors for the oxidation tests were constructed by filling 110 mL amber glass bottles with 40 grams of moist aquifer soil and 80 mL of CA-amended groundwater. The treatment of CA was initiated by adding to each reactor either $S_2O_8^{2-}$, or $S_2O_8^{2-}$ and NaOH. The initial concentration of $S_2O_8^{2-}$ in each reactor was approximately 85 mM. In the experiments with $Fe^{III}$-ox described in section 2.3, although iron (hydr)oxides can activate persulfate (Siegrist et al, 2011) it was found that the activation of $S_2O_8^{2-}$ by $Fe^{III}$-ox did not occur appreciably at room temperature. Therefore, $S_2O_8^{2-}$ in those experiments was activated by heat. In contrast, the aquifer soil was found to be very reactive with $S_2O_8^{2-}$ even at room temperature, presumably due to the presence of reactive iron mineral phases. Therefore, the experiments with the aquifer soil were conducted at 22 ± 1 ºC. The reactors to which only $S_2O_8^{2-}$ was added were denoted as the matrix-activated $S_2O_8^{2-}$ reactors (i.e., the persulfate activators in these reactors were those already present in the soil and groundwater matrix); the initial solution pH in these reactors were between 5 – 6. The reactors that had both $S_2O_8^{2-}$ and NaOH were denoted as base-activated persulfate reactors; the initial pH in these reactors were between 12 – 12.5. The reactors were mixed end-over-end every few hours throughout the course of the experiment. At predetermined time intervals, a 3-mL aliquot was subsampled from the reactors, filtered, and analyzed for pH,

persulfate, and chlorendic acid. The experiment was terminated when more than 95% of the initial persulfate was consumed.

**2.6 Analytical methods.** Filtered samples were acidified to pH 2 and immediately analyzed for chlorendic acid using a Thermo Scientific Ultimate 3000 ultra-high performance liquid chromatograph (UHPLC). The stationary phase was a $C_{18}$ column (Thermo Scientific), while the mobile phase consisted of 70% acetonitrile and 30% 1 mM $H_2SO_4$ which passed through the column at a flow rate of 0.8 mL/min. The UHPLC was equipped with a UV/vis photodiode array detector, and chlorendic acid was detected using UV absorbance at 220 nm. Quantitation of CA in each sample was based on a 5-point calibration curve ($R^2 > 0.99$) established by employing 1 – 100 μM CA standard solutions. TOC was measured on a Shimadzu organic carbon analyzer. Chloride ($Cl^-$) was analyzed on a Thermo Aquion Ion Chromatograph equipped with a suppressed conductivity detector. Persulfate was measured spectrophotometrically using the Kolthoff potassium iodide method (Kolthoff and Belcher, 1957).

All experiments were conducted at least in triplicate, and average values with one standard deviation are reported.

ACCEPTED MANUSCRIPT

## 3. Results and discussion

**3.1 Reactivity of CA with $^{\bullet}OH$ and $SO_4^{\bullet-}$ radicals.** Typical kinetic data obtained from the electron pulse radiolysis experiments are presented in Figures 1 and 2. Based upon the known temperature-dependent value of $k_1$ (Ea = 15.80 kJ $mol^{-1}$) (Gleason *et al.*, 2017) we can calculate the temperature-dependent $k_2$ values of interest, as shown in the inset of Figure 1a. Our calculated rate constant of $k_2 = (8.71 \pm 0.17)\times10^7$ $M^{-1}$ $s^{-1}$ at 24.5 $^{o}$C is over an order of magnitude lower than previously reported by Shah *et al*. who obtained $k = 1.75\times10^9$ $M^{-1}$ $s^{-1}$ through measurement of CA loss using para-chlorobenzoic acid (pCBA) as a stable-product competitor for the $^{\bullet}OH$ radical (Shah et al., 2016). However, this previous approach does not account for any secondary reactions of formed transient species that could also degrade chlorendic acid, which would give an artificially high apparent rate constant. The lower $k_2$ value of this study is consistent with other $^{\bullet}OH$ radical reactions with highly chlorinated species reported in the literature (e.g., the rate constant between endrin and $^{\bullet}OH$ is $k = (2.7 \pm 0.7)\times10^8$ $M^{-1}$ $s^{-1}$ (Haag and Yao, 1992). Mechanistically, it is believed that the oxidation of CA by $^{\bullet}OH$ would take place via H-atom abstraction from the highly sterically-hindered C-H moieties from the ring-joining carbon atoms.

For the reaction between CA and $SO_4^{\bullet-}$, our calculated rate constant at 24.5 $^{o}$C is $k_4 = (6.57 \pm 0.83)\times10^7$ $M^{-1}$ $s^{-1}$, which is also over an order of magnitude lower than the value measured by Shah *et al*. ($k = 2.05\times10^9$ $M^{-1}$ $s^{-1}$) (Shah et al., 2016). The $SO_4^{\bullet-}$ radical reaction could again occur by H-atom abstraction from the same C-H bonds as for $^{\bullet}OH$, but there might be some additional reactivity by electron-abstraction from the negative (deprotonated) carboxylic acid groups in CA.

The reaction rate constant values measured in the temperature range 24.5-70.0 $^{o}$C were used to generate the Arrhenius plots (Insets of Figures 1a and 2a), from which the activation energies for reactions (2) and (4) can be obtained ($E_2$ = 25.43 ± 0.36 and $E_4$ = 37.66 ± 0.33 kJ mol$^{-1}$, respectively). All our kinetic data are summarized in Table 1. To our knowledge, our study is the first that has measured $SO_4^{\bullet-}$ radical kinetics at these elevated temperatures. The experimental setup that we developed (see section 2.2) can be used to generate temperature-dependent rate constants for the reactions between $SO_4^{\bullet-}$ radical and other contaminants and solutes, and this information will be invaluable for understanding and designing heat-activated persulfate treatment systems.

**3.2 Chlorendic acid oxidation in homogeneous system.** In homogeneous solutions containing $S_2O_8^{2-}$ and CA, the most rapid removal of CA was observed at pH 3.6, while the removal at pH 12.2 was the slowest (Figure 3). After 10 hours, over 95% of the initial CA was destroyed at pH 3.6, 55%-60% at pH 8.3, and 25% at pH 12.2. TOC decreased by approximately 25% at pH 8.3 (Figure S2). No CA loss was observed in the absence of $S_2O_8^{2-}$ (data not shown); therefore, the CA loss in the presence of $S_2O_8^{2-}$ was attributable to reactions with $SO_4^{\bullet-}$ and $^{\bullet}$OH, which were produced from the thermal activation of persulfate. Both $SO_4^{\bullet-}$ and $^{\bullet}$OH radicals have been shown to be capable of oxidizing CA (Shah *et al*., 2016; Stowell and Jensen, 1991; Hermes and Knupp, 2015). According to Liang and Su (Liang and Su, 2009) who investigated the activation of persulfate at 70 $^{o}$C, $SO_4^{\bullet-}$ was the predominant oxidant at acidic pH, both $^{\bullet}$OH and $SO_4^{\bullet-}$ were important at neutral pH, and $^{\bullet}$OH was the predominant oxidant at alkaline pH. Therefore, in the current study it is believed that the predominant oxidant responsible for the CA oxidation would be $SO_4^{\bullet-}$ for the pH 3.6 solution, $^{\bullet}$OH in the pH 12.2 solution, and both $SO_4^{\bullet-}$ and $^{\bullet}$OH in the pH 8.3 solution

As with the CA loss rate, the $S_2O_8^{2-}$ utilization efficiency (i.e., E = ($\Delta$[CA]/$\Delta$[ $S_2O_8^{2-}$])×100%) also decreased with increasing pH (Table 2). Possible explanation for the trends between the solution pH and the rate and efficiency include 1) CA is more reactive with $SO_4^{\bullet-}$ than with $^{\bullet}OH$; (note that at 70 ºC $SO_4^{\bullet-}$ is only slightly more reactive than $^{\bullet}OH$, as can be seen from Table 1), 2) CA is more amenable to oxidation at acidic pH, and 3) the scavenging of $SO_4^{\bullet-}$ and $^{\bullet}OH$ by other solutes in the solution (e.g., $S_2O_8^{2-}$, the byproducts of CA oxidation such as $Cl^-$ and other lower molecular-weight compounds) is more pronounced under circumneutral and alkaline conditions.

As the degradation of CA proceeded, the concentration of $Cl^-$ in the solution gradually increased (Figure 3). The production of $Cl^-$ from the oxidation of CA by $SO_4^{\bullet-}$ and $^{\bullet}OH$ was also observed in previous studies. Since each CA molecule contains 6 Cl atoms, the maximum possible value for the ratio $\Delta Cl^-/\Delta$[CA] should be 6. In our study, this ratio was always greater than 5, and approached 6 by the end of the experiment (Table 2). In the pH 8.3 and 12.2 solutions, the $\Delta Cl^-/\Delta$[CA] ratios were also approaching 6 even though over 60% of CA remained in the solution at the end of the experiment. Jensen and coworkers investigated the degradation of CA by ozone ($O_3$) in two separate studies. We calculated the $\Delta Cl^-/\Delta$[CA] ratio in these studies, using Figure 6 in Stowell and Jensen (Stowell and Jensen, 1991) and Figure 2 in Sebastian et al (Sebastian *et al*. 1996), In the first study, $\Delta Cl^-/\Delta$[CA] gradually increased and was 5.5 when 85% of the initial CA was removed, whereas in the second study $\Delta Cl^-/\Delta$[CA] increased to 5.5 when the removal of CA was only 26%. These results and ours suggest that the Cl-containing intermediates produced from the oxidation of CA by $SO_4^{\bullet-}$ and $^{\bullet}OH$ must have been further transformed via the same reaction mechanisms that liberated most of the Cl into the solution as free $Cl^-$. It is noted that although $Cl^-$ ions can be further oxidized into $ClO_3^-$ by $SO_4^{\bullet-}$ and $^{\bullet}OH$ (Lutze *et al.*, 2015), no $ClO_3^-$ was detected in our experiments. Currently, there is very little

information about the mechanisms of CA transformation. Shah et al proposed that the first step of the transformation of CA by $SO_4^{\bullet-}$ and $^{\bullet}OH$ would generate chlorendic anhydride (Shah *et al.*, 2016). However, it is noted that the presence of chlorendic anhydride in their Gas Chromatography analysis is more likely the result of the thermal dehydration of CA in the GC injection port, which was set at T = 250 ºC. The mechanism through which $SO_4^{\bullet-}$ and $^{\bullet}OH$ react with CA, and the byproducts produced are interesting research topics which merit further investigation.

**3.3 Chlorendic acid oxidation and adsorption in the presence of $Fe^{III}$-ox.** A previous study reported that CA could be adsorbed by iron hydroxide precipitates (Ying *et al.*, 1988). The adsorption of CA on iron-containing minerals could significantly influence the ability of $S_2O_8^{2-}$ to destroy CA during ISCO because $SO_4^{\bullet-}$ and $^{\bullet}OH$ are generally not effective at reacting with adsorbed species. Figures 4a and 4c present the fractions of CA in the solution and on the $Fe^{III}$-ox surface (50 g/L) during the treatment with persufate at T = 70 ºC. As with the homogeneous experiment, our intention was to investigate the removal of CA under acidic, circumneutral, and alkaline conditions. However, in the experiment with initial pH of 4, the pH of the solution quickly increased to pH 6 after 1 hour, and from there gradually increased to pH 7.1 by the end of the experiment. Because the decomposition of $S_2O_8^{2-}$ produces $H^+$, which should have caused the pH of the solution to decrease, the pH increase in this experiment was attributable to the ability of $Fe^{III}$-ox to buffer the solution in the circumneutral pH range. Therefore, although the solution in this experiment was initially acidic, the experiment is referred to as the circumneutral pH experiment in the subsequent discussion.

Under the circumneutral pH condition, except for t = 0 h the adsorbed fraction accounted for over 50% of the total CA in the system (Figure 4a). In contrast, only less than 5% of the CA in

the pH 12.2 experiment was associated with $Fe^{III}$-ox (Figure 4c). Under both pH regimes, the total concentration of CA decreased over time (Figures 4b and 4d), although the rates of decrease were slower than those in the respective pH regime of the homogeneous systems (Figures 3b and 3c). The stoichiometric efficiencies, E, in the homogeneous and heterogeneous systems were comparable at circumneutral pH, whereas at alkaline pH the efficiency in the heterogeneous system was almost three times lower than that in the homogeneous system (Table 2). It is noted that since only approximately 90% of the CA adsorbed on $Fe^{III}$-ox could be recovered by extraction (see section 2.4), the actual E in the heterogeneous system could be slightly lower than the values reported in Table 2. It is also noted that although $Cl^-$ was measured in the heterogeneous experiment (Figure 4b and 4d), the concentration at each sampling point represented the total $Cl^-$ released from CA and the $Cl^-$ leached from impurities in $Fe^{III}$-ox. (The presence of $Cl^-$-containing impurities in $Fe^{III}$-ox was confirmed by washing $Fe^{III}$-ox particles and measuring $Cl^-$ in the spent solution). The contribution of $Cl^-$ by the impurities explains why some $\Delta Cl^-/\Delta[CA]$ values were greater than 6 (Table 2).

The slower CA oxidation and lower E in the heterogeneous system are attributable to 1) the slower rate of $S_2O_8^{2-}$ decomposition (compare the inset of Figures 3b vs. 3b, and 3c vs. 4d), which resulted in the slower rates of $SO_4^{\bullet-}$ and $^{\bullet}OH$ production; 2) the scavenging of $SO_4^{\bullet-}$ and $^{\bullet}OH$ by the $Fe^{III}$-ox surface; since CA is only moderately reactive with $SO_4^{\bullet-}$ and $^{\bullet}OH$ ($k_{OH}$ and $k_{SO4} < 5\times10^8\ M^{-1}s^{-1}$), introducing any scavenger into the system ($Fe^{III}$-ox in this case) would have appreciably slowed the oxidation of CA; and 3) the adsorption of CA on $Fe^{III}$-ox, which would reduce the amount of dissolved CA available for reacting with $SO_4^{\bullet-}$ and $^{\bullet}OH$. In the pH 12.2 experiment, the adsorption should not appreciably affect CA oxidation since most CA remained in the solution. In the circumneutral pH experiment, since over 50% of the CA in the system was

340 associated with $Fe^{III}$-ox, the oxidation of CA by $SO_4^{\bullet-}$ and $^{\bullet}OH$ must have been influenced, at
341 least in part, by the adsorption/desorption of CA.

ACCEPTED MANUSCRIPT

**3.4 Effect of pH on CA adsorption on model minerals.** To further investigate the influence of adsorption on the fate of CA, the affinity of CA to $Fe^{III}$-ox as well as to other model minerals such as $MnO_2$, $Al_2O_3$, and $SiO_2$ was investigated in solutions with pHs ranging from 2 to 12. The fraction of CA that adsorbed onto $Fe^{III}$-ox decreased with increasing pH (Figure 5). At pH < 2.5, essentially all CA in the system was associated with $Fe^{III}$-ox regardless of the solid concentration (i.e., 5 g/L vs. 50 g/L). In contrast, over 95% of CA remained in the solution when pH was greater than 10. Not surprisingly, in the pH range 2.5 – 10 more CA was adsorbed by 50 g/L $Fe^{III}$-ox than by 5 g/L $Fe^{III}$-ox. A similar trend between pH and CA adsorption was also observed by Ying *et al*, who reported that more CA was adsorbed on ferric hydroxide precipitates at pH 3.3 than at pH 7 (Ying *et al*, 1988). In the presence of 50 g/L of $Fe^{III}$-ox, the fraction of CA associated with $Fe^{III}$-ox at pH 8.3 was approximately 20-25%. In the oxidation experiment conducted at the same pH, the fraction of CA associated with $Fe^{III}$-ox was 10% at t = 0h, and was over 50% at the other time points (Figure 4a). However, direct comparison of the fraction of CA adsorbed in these two experiments is not possible since the experiments were conducted at different temperature (i.e., T = 22 ºC in the adsorption experiment vs. T = 70 ºC in the oxidation experiment), and employed solutions with different composition (i.e., the solutions in the adsorption experiment did not contain $S_2O_8^{2-}$).

Similar trends between pH and CA adsorption were observed with $SiO_2$, $MnO_2$, and $Al_2O_3$, although compared to the adsorption edges of $Fe^{III}$-ox and $Al_2O_3$, those of $SiO_2$ and $MnO_2$ were displaced toward more acidic pH (Figure 6). In the case of $Al_2O_3$, the decrease in adsorption between pH 2.5 and 4.5 was attributable to the dissolution of $Al_2O_3$ in this pH range. Based on the adsorption edge trends among the solids, and the trend between adsorption and pH, it is hypothesized that the adsorption of CA is controlled by electrostatic interactions between the

surface and CA molecules. Above the point of zero charge (pzc) of each solid (i.e., 2 – 5 for $SiO_2$, 3 – 6 for $MnO_2$ and 7.5 – 9 for $Al_2O_3$ and iron oxides) (Sverjensky and Sahai, 1996, Sahai and Sverjensky, 1997, Cristiano *et al.*, 2011), both CA ($pK_{a1}$ = 3.1, $pK_{a2}$ = 4.6) and the surface are negatively charged. As the pH increased, the surface becomes more negatively charged, resulting in an increase in repulsion between CA and the surface, and therefore a decrease in CA adsorption. In the pH range between $pK_{a1}$ and pzc, the negatively charged CA molecule would be attracted to the positively charge surface. At pH < $pK_{a1}$, the CA molecules that are negatively charged would be electrostatically attracted to the positively charged surface, whereas the CA molecules that are neutrally charged could have some affinity towards the surface due to the non-specific interaction (i.e., hydrophobic-hydrophobic interaction).

Overall, the results described above indicate that the groundwater pH and the geology of the subsurface could have significant influence on the mobility of CA in the subsurface, as well as the ability of activated-$S_2O_8^{2-}$ to destroy CA during ISCO.

**3.5 Experiments with groundwater and aquifer soil.** In the homogeneous and heterogeneous experiments (sections 3.2 and 3.3), the initial concentration of $S_2O_8^{2-}$ was 1 mM (0.192 g/L as $S_2O_8^{2-}$). This concentration is relatively low compared to the concentrations of $S_2O_8^{2-}$ solutions used in remedial systems, which typically ranges between low and high tens of grams per liter of $S_2O_8^{2-}$. Once introduced into the subsurface $S_2O_8^{2-}$ will be activated into $SO_4^{\bullet-}$ and $^{\bullet}OH$ by aquifer soil, or by solutions containing dissolved metals or a strong base that are co-injected with $S_2O_8^{2-}$. $S_2O_8^{2-}$ can also be activated *in situ* by heat via steam injection, addition of $H_2O_2$ (the decomposition of $H_2O_2$ liberates heat), or electrical resistance heating (Tsitonaki *et al.*, 2010; Reynolds, 2014). With base activation the solution pH usually remains at above pH 10, whereas with the other activation techniques the solution pH can decrease to as low as pH 2 – 3 once the

natural buffering capacity of the subsurface is depleted. This is because the decomposition of each $S_2O_8^{2-}$ molecule generates two $H^+$ ions.

Because CA adsorption is influenced by the solution pH (Figures 5 and 6), the fluctuation of pH in $S_2O_8^{2-}$-based remedial systems can significantly affect the oxidative treatment of CA. To further examine the utility of $S_2O_8^{2-}$ for *in-situ* treatment of CA, the degradation of CA in reactors containing authentic samples of groundwater and aquifer soils was conducted. A preliminary experiment conducted at 70 ºC showed that the combination of heat and matrix activations resulted in a rapid pH decrease to < 2 and a 100% loss of CA due to adsorption within only 15 minutes (data not shown). As such, all experiments with groundwater and aquifer soil were conducted at 22 ± 1 ºC and not at elevated temperature, as in the experiments with $Fe^{III}$-ox.

In the matrix-activated persulfate reactors, as the decomposition of persulfate took place, the solution pH dropped from 5.5 to 1.7 within the first 18 hours of the experiment. Concurrently, CA levels dropped below our detection limit (<1 μM) (Figure 7). However, CA concentrations rebounded to near baseline conditions when the pH of the solution was adjusted back to pH ~ 6. A similar CA concentration-pH trend was observed in the subsequent 50 hours, with CA concentrations decreasing in the solution as the pH decreased but increasing again as the pH was raised. This CA concentration trend is attributable to the CA adsorption on and desorption from the aquifer soils. This hypothesis is supported by an adsorption test, which revealed that all CA was associated with the aquifer soils at pH below 2.5, whereas over 90% CA remained in the solution at pH above 6 (Figure 8). In the reactors containing $S_2O_8^{2-}$, the oxidation of CA did not occur to an appreciable extent (Figure 7); in fact, only less than 3% of CA was oxidized after more than 95% of $S_2O_8^{2-}$ was consumed (E < 0.003%).

Neither adsorption nor oxidative transformation of CA occurred appreciably in the base-activated $S_2O_8^{2-}$ reactors (Figure 7). The adsorption of CA did not take place as the pH of the solution in these reactors was maintained at above 12 throughout the experiment, whereas the lack of oxidative transformation is attributable to the radical scavenging by the aquifer soil surface (the aquifer soil contained 0.4 mg/kg of organic carbon), as well as by groundwater solutes such as $CO_3^{2-}$, $Cl^-$, and dissolved organic matter.

## 4. Conclusions and implications for the remediation of CA by $S_2O_8^{2-}$

Based on the findings described above, the following conclusions can be made about the *in-situ* remediation of CA. Firstly, due to the affinity of CA toward surfaces, the groundwater pH and the geology of the subsurface could have a significant influence on the mobility of CA and the extent of the CA plume. Secondly, activated persulfate can be used to oxidize CA. However, given the moderate reactivity of CA with $SO_4^{\bullet-}$ and $^{\bullet}OH$ radicals ($k_{SO4} = (6.57 \pm 0.83)\times10^7\ M^{-1}s^{-1}$ and $k_{OH} = (8.71 \pm 1.67)\times10^7\ M^{-1}s^{-1}$ at 24.5 $^oC$), the oxidation of CA will only occur appreciably when radical scavengers such as background solutes, dissolved organic matter, and co-contaminants are not present in significant quantities. Thirdly, in the presence of a surface, adsorption is expected to be the predominant mechanism of CA removal under acidic conditions. As such, the disappearance of CA (if observed) following the injection of $S_2O_8^{2-}$ should be carefully scrutinized, because such disappearance could be the result of adsorption rather than oxidative transformation. The adsorption of CA on aquifer soils can be particularly significant in systems with low pH buffering capacity where the pH can drop dramatically as $S_2O_8^{2-}$ decomposes. When adsorption is the primary removal mechanism, the concentration of CA in the groundwater is expected to rebound once pH increases and desorption starts to occur. While monitoring the concentration of $Cl^-$ in the groundwater may help determine if oxidative

434 transformation is occurring (since the transformation of CA generates $Cl^-$), it will be difficult to
435 detect changes in systems containing a high concentration of background $Cl^-$. Fourthly, the
436 transformation of CA could take place in systems where the solution pH remains neutral
437 throughout the treatment, such as in systems containing excess buffering capacity (e.g., Figure
438 3b). However, such systems will likely contain high concentrations of bicarbonate and carbonate
439 which can compete with CA for $^{\bullet}OH$ and $SO_4^{\bullet-}$. Finally, under alkaline conditions typical of
440 remedial systems in which $S_2O_8^{2}$ is activated by a base, CA would remain in the solution and
441 would be available for reacting with $^{\bullet}OH$ and $SO_4^{\bullet-}$. However, as in the circumneutral systems,
442 the CA transformation rate and efficiency are expected to be low due to the scavenging of the
443 radicals by aquifer soils and the solutes present in the groundwater.

444 When $S_2O_8^{2-}$ is deemed to be ineffective, other remedial options for CA could potentially be
445 *in-situ* transformation by a strong reductant (e.g., zero-valent iron), or adsorptive *ex situ*
446 treatment (i.e., pump-and-treat). The ability of zero-valent iron to destroy CA is currently being
447 evaluated in our laboratory.

448

449 **Acknowledgement.** Funding for this research was provided by Ontario Centres of Excellence
450 (VIP1 Grant #27828), and Natural Sciences and Engineering Research Council of Canada
451 (Discovery Grant #2015-04850). Kinetic measurements were made at the Radiation Research
452 Laboratory, University of Notre Dame, which is funded by the Office of Basic Energy Sciences,
453 U.S. Department of Energy.

ACCEPTED MANUSCRIPT

## References


Boisa, N. Photo-catalytic degradation of chlorendic acid: 1. Degradation products. *Journal of Applied Sciences and Environmental Management*, 2013, 17, 335-340.

Boczkaj, G., Fernandes, A. Wastewater treatment by means of advanced oxidation processes at basic pH conditions: a review. *Chemical Engineering Journal*, 2017, 608-633.

Buxton, G. V., Greenstock, C. L., Helman, W. P., Ross, A. B. Critical review of rate constants for reactions of hydrated electrons, hydrogen atoms and hydroxyl radicals (OH/O-) in aqueous solution. *Journal of Physical and Chemical Reference Data*, 1988, 17, 513−887.

Buxton, G. V., Stuart, C. R. Re-evaluation of the thiocyanate dosimeter for pulse radiolysis. *Journal of Chemical Society Faraday Transactions*, 1995, 91, 279−82.

Cristiano E., Hu, Y., Siegfried, M., Kaplan, D., Nitsche, H. A comparison of point of zero charge measurement methodology. *Clays and Clay Minerals*, 2011, 59, 107-115.

Cochrane W.P., Forbes, M.A. Oxidation products of heptachlor and its metabolites – a chemical study. *Chemosphere*, 1974, 41-46.

Drzewicz, P., Perez-Estrada, L.A., Alpatova, A., Martin, J.W., El-Din, M.G. Impact of peroxydisulfate in the presence of zero valent iron on the oxidation of cyclohexanoic acid and naphthenic acids from oil sands process-affected water. *Environ. Sci. Technol.* 2012, 46, 8984-8991.

Gleason, J. M., Garrett, M., Ishida, K. P., Mezyk, S. P. Temperature dependence of hydroxyl radical reactions with chloramine species in aqueous solution. *Chemosphere*, 2017, 187, 123-129.

Haag, W.R., Yao, C.C.D. Rate constants for reaction of hydroxyl radicals with several drinking-water contaminants. *Environmental Science & Technology*, 1992, 26, 1005-1013.

Hendrix P.F., Hamala, J.A., Langner, C.L., Kollig, H.P. Effects of chlorendic acid, a priority toxic substance, on laboratory aquatic ecosystems. *Chemosphere*, 1983, 1083-1099.

Hermes N., Knupp, G. Transformation of atrazine, bisphenol A and chlorendic acid by electrochemically produced oxidants using a lead dioxide electrode. *Environmental Science: Water Research & Technology*, 2015, 1, 905-912.

Hug, G.L., Wang, Y., Schoneich, C., Jiang, P.-Y., Fessenden, R.W., Multiple time scales in pulse radiolysis. Application to bromide solutions and dipeptides. *Radiation Physics and Chemistry*, 1999, 54, 559-566.

Huling, S. G., Pivetz, B. E., 2006. In-Situ Chemical Oxidation. *U.S. Environmental Protection Agency Engineering Issue.* https://archive.epa.gov/ada/web/html/isco.html.

IPCS, 1996. Chlorendic acid and anhydride. World Health Organization.

Kolthoff, I. M., Belcher, R. Titration methods: oxidation-reduction reactions, vol. III, John Wiley & Sons, Inc, New York (1957), pp. 287-291.

Liang C., Su, H. Identification of sulfate and hydroxyl radicals in thermally activated persulfate. *Ind. Eng. Chem. Res.*, 2009, 48, 5558-5562.

Lutze, H. V., Kerlin, N., Schmidt, T. C. Sulfate radical-based water treatment in the presence of chloride: formation of chlorate, inter-conversion of sulfate radicals into hydroxyl radicals and influence of bicarbonate. *Water Research*, 2015, 72, 349-360.

NTP, 1987. NTP toxicology and carcinogenesis studies of chlorendic acid (CAS No. 115-28-6) in F344/N rats and B6C3F1 mice (feed studies). Natl. Toxicol. Program Tech. Rep. Ser. 1987, 304, 1-225.

Oman, C., Hynning, P. Identification of organic compounds in municipal landfill leachates. *Environmental Pollution*, 1993, 265-271.

Reynolds, D. A., 2014. United States Patent 9004816 B2.

Sebastian J.H., Weber, A. S., Jensen, J. N. Sequential chemical/biological oxidation of chlorendic acid. *Water Research*, 1996, 30, 1833-1843.

Sahai N., Sverjensky, D. Evaluation of internally consistent parameters for the triple-layer model by the systematic analysis of oxide surface titration data. *Geochimica et Cosmochimica Acta*., 1997, 2801-2826.

Shah, N.S., Khan, J. A., Al-Muhtaseb, A. H., Sayed, M., Murtaza, B., Khan, H. M. Synergistic effects of $HSO_5^-$ in the gamma radiation driven process for the removal of chlorendic acid: a new alternative for water treatment. *Chemical Engineering Journal*, 2016, 306, 512-521.

Siegrist, R. L., Crimi, M., Simpkin, T. J., 2011. In situ chemical oxidation for groundwater remediation. Springer, NY.

Spinks, J. W. T., Woods, R. J. An Introduction to Radiation Chemistry; John Wiley & Sons: New York, 1990.

Stowell, J. P., Jensen, J. N. Dechlorination of chlorendic acid with ozone. *Water Research*, 1991, 25, 83-90.

Sverjensky, D., Sahai N. Theoretical prediction of single-site surface-protonation equilibrium constants for oxides and silicates in water. *Geochimica et Cosmochimica Acta.* 1996, 60, 3773-3797.

Sverko, E., Tomy, G.T., Reiner, E.J., Li, Y., McCarry, B.E., Arnot, J.A., Law, R.J., Hites, R.A. Dechlorane plus and related compounds in the environment: a review. *Env. Sci. Technol.* 2011, 45, 5088-5098.

Tsitonaki, A., Petri, B., Crimi, M., Mosbæk, H., Siegrist, R. L., Bjerg, P. L. In situ chemical oxidation of contaminated soil and groundwater using persulfate: a review. *Critical Reviews in Environmental Science and Technology*, 2010, 40, 55-91.

Whitman, K., Lyons, S., Miller, R., Nett, D., Treas, P.. Zante, A., Fessenden, R. W., Thomas, M. D., Wang, Y. Linear accelerator for radiation chemistry research at Notre Dame 1995. In Proceedings of the '95 Particle Accelerator Conference and International Conference on High Energy Accelerators, Dallas, TX, 1996.

Ying, W., Bonk R.R., Lloyd V.J., Sojka, S.A. Biological Treatment of a Landfill Leachate in Sequencing Batch Reactors. *Environmental Progress*, 1986, 41-50.

Ying, W., Duffy, J.J., Tucker, M. E. Removal of Humic Acid and Toxic Organic Compounds by Iron Precipitation. *Environmental Progress*, 1988, 262-269.

| Temp (°C) | $k_{OH}$ ($M^{-1}s^{-1}$) | $k_{SO4}$ ($M^{-1}s^{-1}$) |
|---|---|---|
| 24.5 | $(8.71 \pm 0.17) \times 10^7$, $R^2 = 0.997$ | $(6.57 \pm 0.83) \times 10^7$, $R^2 = 0.983$ |
| 40 | $(1.48 \pm 0.11) \times 10^8$, $R^2 = 0.979$ | $(1.42 \pm 0.20) \times 10^8$, $R^2 = 0.945$ |
| 70 | $(3.41 \pm 0.12) \times 10^8$, $R^2 = 0.995$ | $(4.96 \pm 0.31) \times 10^8$, $R^2 = 0.977$ |

**Table 1.** Temperature-dependent rate constant for the reactions between CA and hydroxyl or sulfate radicals. All solutions were buffered with 10 mM phosphate to give an initial pH of 7.0.

| pH initial | pH final | $E = (\Delta[CA]/\Delta[S_2O_8^{2-}])\times 100\%$ | | $\Delta[Cl^-]_{produced}/\Delta[CA]$ | |
|---|---|---|---|---|---|
| | | t = 4h | t = 10h | t = 4h | t = 10h |
| 3.6 | 2.7 | 15.2% | 11.5% | 5.1 | 5.6 |
| 8.3 | 8.4 | 6.7% | 6.4% | 5.2 | 5.9 |
| 12.2 | 11.8 | 5.4% | 3.5% | 5.3 | 5.8 |
| 4-5.5 | 7.1 | 7.2%* | 6.1%* | 6.6** | 7.4** |
| 12.2 | 10 | 1.9%* | 1.3%* | 11.7** | 12.6** |

**Table 2.** Persulfate utilization efficiency E and $\Delta[Cl^-]_{produced}/\Delta[CA]$ in the homogeneous (the first three rows) and heterogeneous (the last 2 rows) oxidation of CA by persulfate.

* The actual efficiency might be slightly lower, as only ca. 90% of the adsorbed CA can be recovered from the iron oxide surface.

** As each CA molecule contains 6 Cl atoms, the maximum theoretical value for $\Delta[Cl^-]_{produced}/\Delta[CA]$ should be 6. The higher values observed in these experiments are likely due to the contribution of $Cl^-$ impurity released from the iron oxide.

ACCEPTED MANUSCRIPT

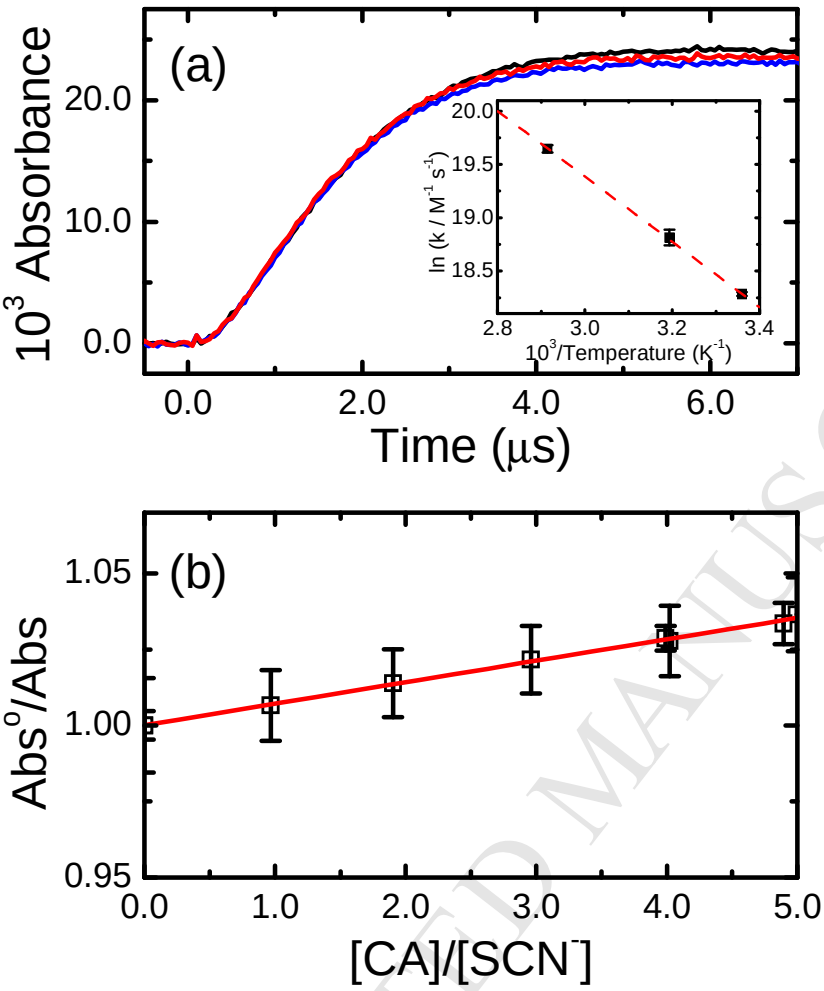


**Figure 1.** (a) Typical data obtained for $(SCN)_2^{-\bullet}$ transient absorbance growth kinetics at 475 nm for 100.0 μM KSCN in $N_2O$-saturated, pH 7.00, water containing zero (black, top), 96.6 μM (red, middle) and 499.4 μM (blue, bottom) chlorendic acid at 24.5°C. (b) Transformed competition kinetics plot for hydroxyl radical reaction with chlorendic acid using $SCN^-$ as a standard. Solid line is weighted linear fit corresponding to reaction rate constant of $k_2$ = (8.71 ± 0.17) x $10^7$ $M^{-1}$ $s^{-1}$ at this temperature. Inset in (a): Arrhenius plot for measured $k_5$ rate constant over the range 24.5 – 70.0 °C (see values in Table 1). Fitted line corresponds to activation energy of $E_2$ = 25.43 ± 0.36 kJ $mol^{-1}$.

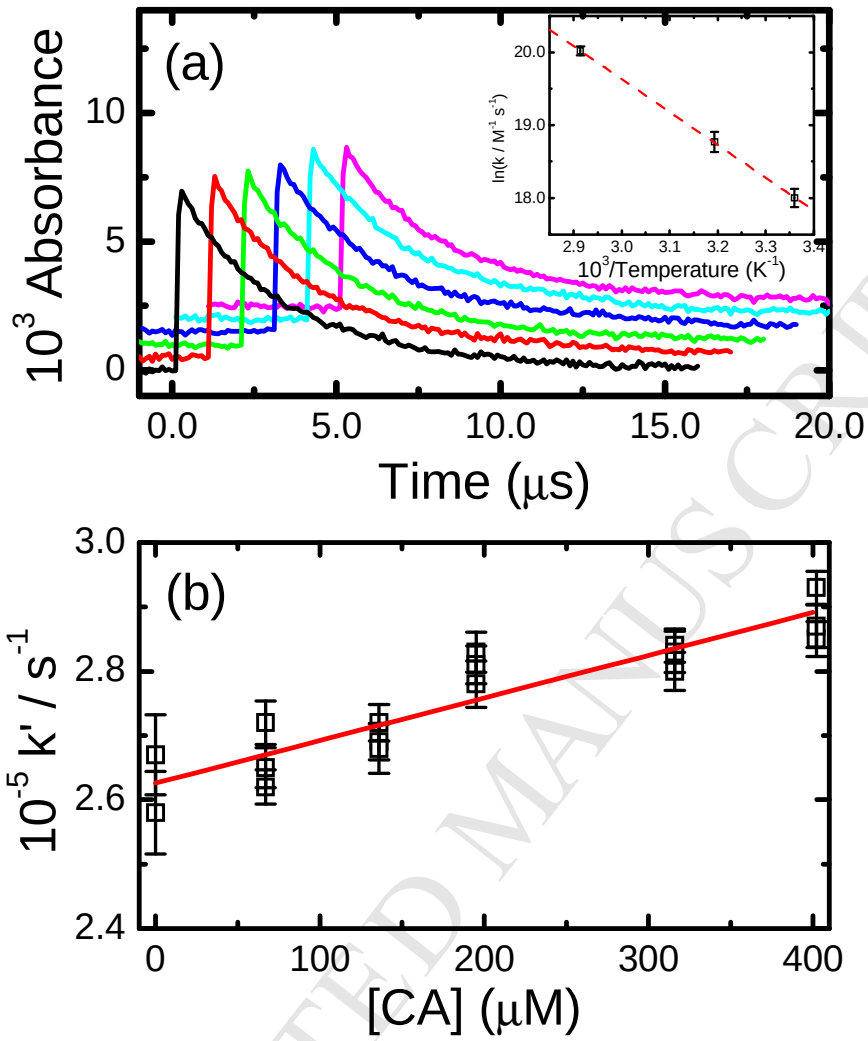


**Figure 2.** (a) Typical kinetic data obtained for $SO_4^{\bullet-}$ radical decay at 450 nm in aerated 0.10 M $K_2S_2O_8$ solution at pH 7.0 and 24.5°C. Kinetic traces have been offset in time and intensity to aid visibility. From left to right, kinetic traces correspond to zero (black, lower left), 67 (red), 136 (green), 196 (dark blue), 315 (light blue), and 402 (magenta) μM added CA. (b) Second-order rate constant determination for Reaction (4) was based upon first-order, exponential, fits to the kinetic data of (a). Solid line corresponds to $k_4 = (6.57 \pm 0.83) \times 10^7$ M$^{-1}$ s$^{-1}$. Inset in (a): Arrhenius plot of kinetic data obtained over the temperature range 24.5–70.0°C. The fitted line gives Arrhenius activation energy of $E_4 = 37.66 \pm 0.33$ kJ mol$^{-1}$.

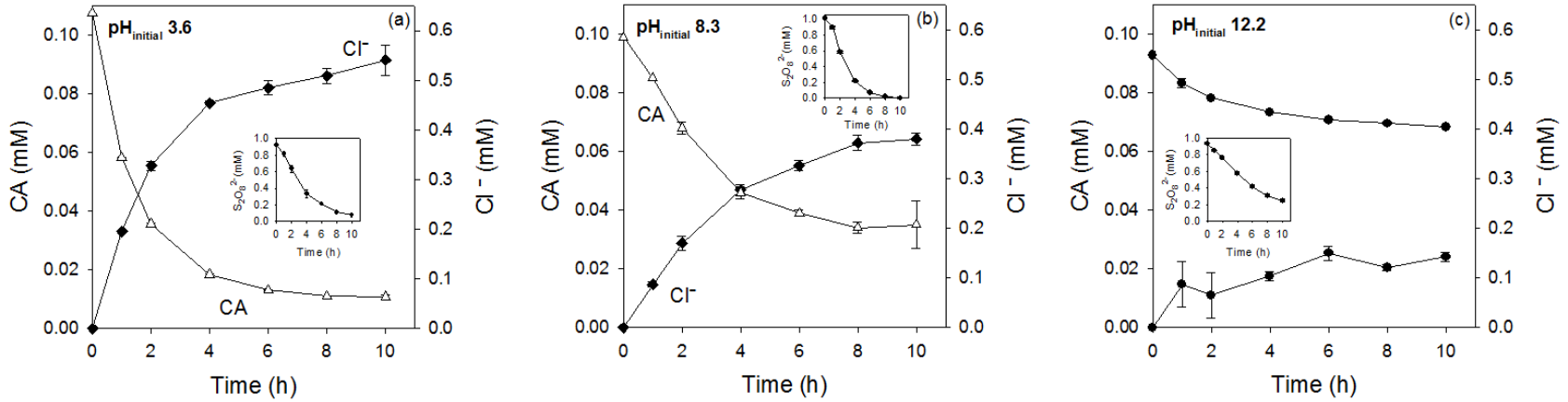


**Figure 3.** Decomposition of persulfate, degradation of CA, and production of chloride in solid-free solution**.** $[S_2O_8^{2-}]_0$ = 1 mM, $[CA]_0$ = 0.095 – 0.105 mM, T = 70 ºC, $[Na_2SO_4]$ = 50 mM (background electrolyte). **A**. pH $_{initial}$ = 3.6, pH $_{final}$ = 2.7 (no buffer); **B**. pH $_{initial}$ = 8.3, pH $_{final}$ = 8.4, the solution was buffered by 20 mM borate; **C**. pH $_{initial}$ = 12.2, pH $_{final}$ = 11.8 (no buffer).

ACCEPTED MANUSCRIPT

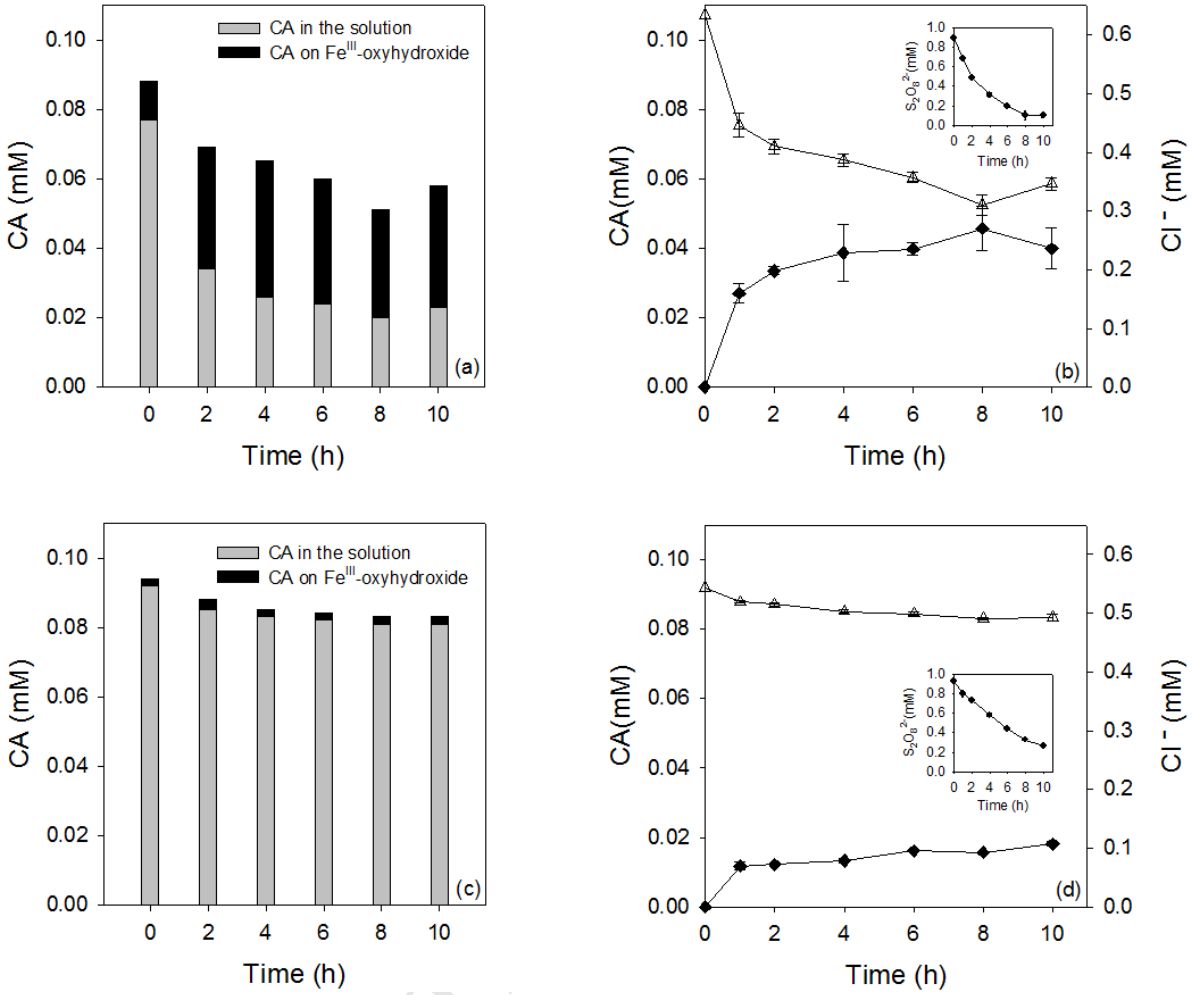


**Figure 4.** Oxidation of CA by persulfate in solution containing 50 g/L of $Fe^{III}$-oxyhydroxide. (a) and (c): Amounts of soluble CA and adsorbed CA over the course of the experiment; (b) and (d): concentration-time profiles of CA (soluble + adsorbed), persulfate, and chloride. $[S_2O_8^{2-}]_0$ = 0.95-1 mM, $[CA]_0$ = 0.095-0.105 mM, $[Na_2SO_4]$ = 50 mM, 70 ºC. (a): Initial pH = 4 – 5.5, final pH = 7.1; (c): Initial pH = 12.2, final pH = 10. (no buffer).

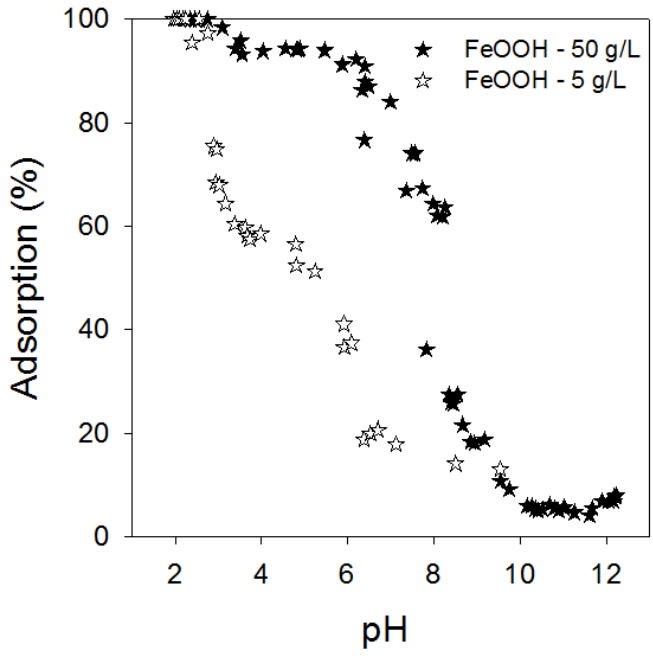


**Figure 5.** Adsorption of CA onto 5 g/L and 50 g/L $Fe^{III}$-oxyhydroxide. $[CA]_0$ = 0.1 mM.

ACCEPTED MANUSCRIPT

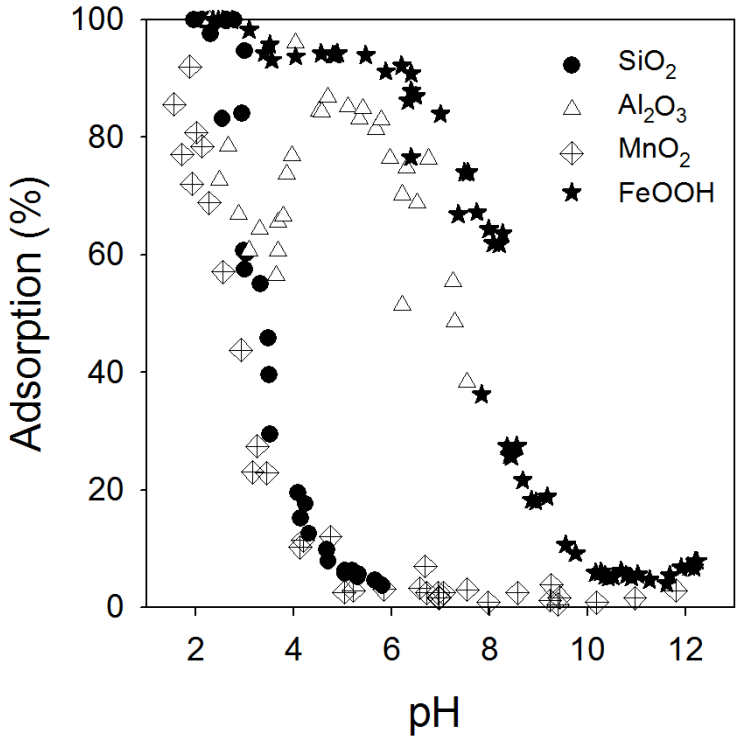


**Figure 6.** Adsorption of chlorendic acid (CA) onto silica, alumina, pyrolusite, and $Fe^{III}$-oxyhydroxide. $[CA]_0$ = 0.1 mM; [solid] = 50 g/L.

ACCEPTED MANUSCRIPT

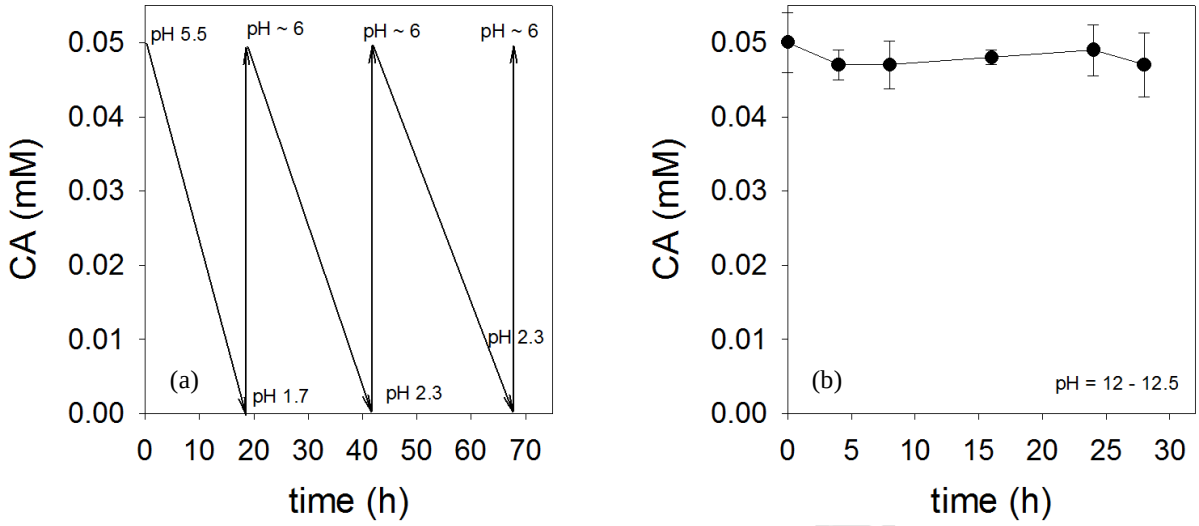


**Figure 7.** Degradation of CA in a solution containing aquifer soil and groundwater. Each reactor contained 40 g soil and 80 mL groundwater. The groundwater was amended with CA such that the initial CA concentration was 0.05 mM. (a) natural-activated persulfate experiment; (b) base-activated persulfate experiment in which the solution pH was maintained between 12 and 12.5 by addition of aliquots of 5 M NaOH. The initial concentration of $S_2O_8^{2-}$ was 85 mM, and the experiments were terminated when over 95% of persulfate was consumed (3 days for the natural-activated persulfate experiment, and 1 day for the base-activated persulfate experiment). Experiments were conducted at T = 22 ºC.

ACCEPTED MANUSCRIPT

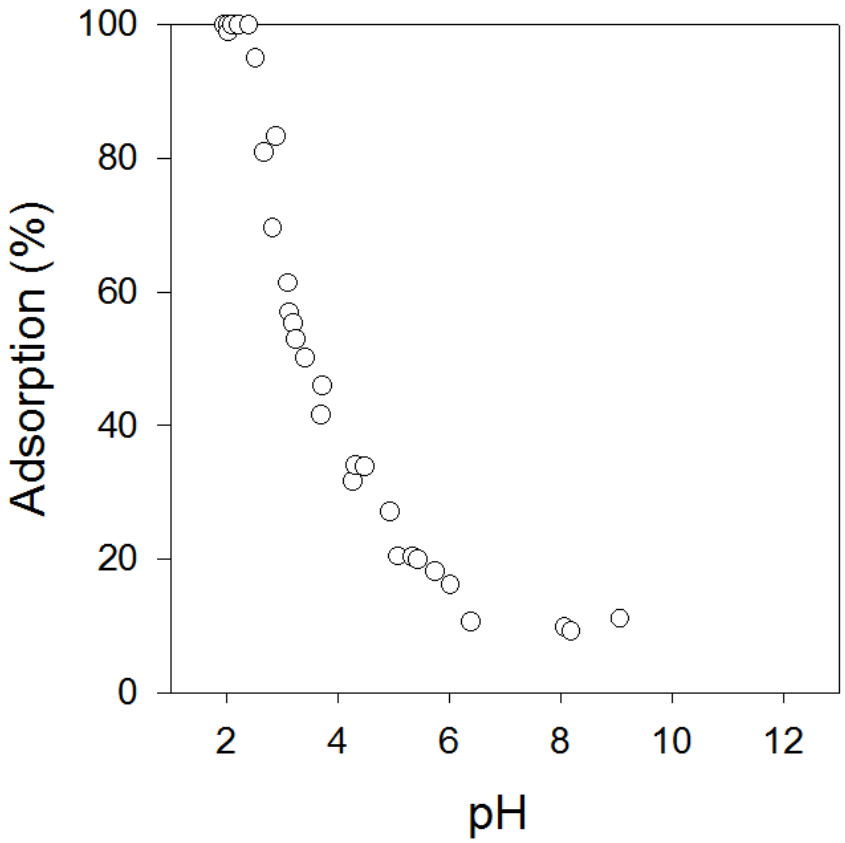


**Figure 8.** Adsorption of chlorendic acid (CA) onto aquifer soil. $[CA]_0$ = 0.05 mM; [solid] = 50 g/L.

ACCEPTED MANUSCRIPT

ACCEPTED MANUSCRIPT

Highlights

- Activated persulfates ($S_2O_8^{2-}$) could degrade CA only under certain conditions
- In homogeneous (i.e., solid-free) solutions, CA could be oxidized by $^{\bullet}OH$ and $SO_4^{\bullet-}$
- In heterogeneous solutions, CA was removed mainly by adsorption to solids
- Adsorption of CA retarded/inhibited the oxidation of CA, especially at acidic pH
- CA desorption after $S_2O_8^{2-}$ is depleted may cause the CA concentration to rebound

ACCEPTED MANUSCRIPT